Heterogeneous Catalysis

International Edition: DOI: 10.1002/anie.201604136
German Edition: DOI: 10.1002/ange.201604136

Unraveling the Catalytic Synergy between Ti^{3+} and Al^{3+} Sites on a Chlorinated Al_2O_3: A Tandem Approach to Branched Polyethylene

*Alessandro Piovano, K. S. Thushara, Elena Morra, Mario Chiesa, and Elena Groppo**

Abstract: *An original step-by-step approach to synthesize and characterize a bifunctional heterogeneous catalyst consisting of isolated Ti^{3+} centers and strong Lewis acid Al^{3+} sites on the surface of a chlorinated alumina has been devised. A wide range of physicochemical and spectroscopic techniques were employed to demonstrate that the two sites, in close proximity, act in a concerted fashion to synergistically boost the conversion of ethylene into branched polyethylene, using ethylene as the only feed and without any activator. The coordinatively unsaturated Al^{3+} ions promote ethylene oligomerization through a carbocationic mechanism and activate the Ti^{3+} sites for the traditional ethylene coordination polymerization.*

In the last years, much research has been devoted to the development of new tandem catalytic approaches to olefin polymerization, which allow the synthesis of polyolefins with tunable properties in a one-pot reaction, using a single olefin feed.[1–4] Tandem catalysis for branched polyethylene synthesis is one of such example. To this aim, two cooperative components are engineered into a single catalyst. One component oligomerizes ethylene to short α-olefins, which are successively incorporated in the growing polyethylene chains through an "in situ branching" mechanism by a second, different, catalytic center.[5–7] This co-monomer-free process for branched polyethylene synthesis opens an attractive atom-efficient scenario, reducing the costs of feedstock, loading, purification, storage, and downstream recycling.

Notable examples of tandem catalysts for olefin polymerization can be found in the field of homogeneous catalysis, in which the catalysts' design has reached unexpected levels of excellence and competes even with some natural enzymes.[8] Intermolecular tandem reactions are efficient only when the two catalytic sites are constrained in close spatial proximity, a condition that allows a rapid enchainment of the α-olefin co-monomers produced at the first site into the polyethylene chains growing at the second site.[9,10]

In this investigation, we have specifically devised an original step-by-step approach to synthesize and characterize a bifunctional heterogeneous catalyst for the production of branched polyethylene using ethylene as the only feed, without any activator. This approach differs from the typical methods in the olefin polymerization field, in which heterogeneous dual-site catalysts are usually obtained by a partial modification of the original catalyst through the intervention of an external agent.[7,11–13] The catalyst is obtained by treating a transitional alumina with $TiCl_4$ and a subsequent H_2 reduction (as was similarly proposed in previous patents,[14,15] but never investigated in details), and benefits from the presence of Ti^{3+} sites in close proximity to exposed Al^{3+} Lewis acid sites on a highly chlorinated surface, each site performing a specific catalytic function. We will demonstrate that the two sites cooperate to give a branched polyethylene. The novelty of our approach lies in the capability to monitor, by means of a multi-technique characterization approach (Diffuse Reflectance (DR) UV/Vis, FT-IR, and continuous wave (CW) and pulse electron paramagnetic resonance (EPR) spectroscopies),[16] each phase of the catalyst synthesis, including the in situ monitoring during ethylene polymerization, thereby enabling structure–property correlations to be established.

The δ-$Al_2O_{3\text{-}600}$/$TiCl_4$ precatalyst was obtained by exposing δ-Al_2O_3 that was dehydroxylated at 600 °C (δ-$Al_2O_{3\text{-}600}$) to $TiCl_4$ vapor at 25 °C, followed by the removal of excess $TiCl_4$. FT-IR spectra collected during the reaction demonstrate that $TiCl_4$ immediately reacts with surface hydroxy groups (spectrum 1 in Figure 1 b), grafting as -$TiCl_x$ onto the alumina surface and releasing HCl. This reaction is similar to the $TiCl_4$ grafting on dehydroxylated silica,[17–21] but alumina has the unique capacity to stabilize the HCl on surface Al^{3+}-O^{2-} acid–base pairs (spectrum 2 in Figure 1 b).[22] DR UV/Vis spectroscopy reveals the presence of a variety of grafted Ti^{4+} sites, having both oxygen and chlorine ligands, and displaying both four-fold and six-fold coordination geometries (spectrum 2 in Figure 1 a and the Supporting Information section 2.2).[23–25]

The δ-$Al_2O_{3\text{-}600}$/$TiCl_4$/$H_{2\text{-}400}$ catalyst was obtained by reducing the precatalyst under H_2 at 400 °C. Under these conditions Ti^{3+}($3d^1$) species are formed, as indicated by X-band CW EPR (Supporting Information, Figure S2) and DR UV/Vis (spectrum 3 in Figure 1 a) spectroscopies. The reaction with O_2 and the subsequent formation of EPR active superoxide radicals demonstrates that at least a fraction of the Ti^{3+} sites present pre-existing coordinative vacancies (Supporting Information, Figure S4).[26] The simultaneous removal of chemisorbed HCl (spectrum 3 in Figure 1 b) leaves an extensively chlorinated surface, as verified by complementary FT-IR experiments (Supporting Information, Figure S1 a). Although the formation of a crystalline $AlCl_3$ phase was excluded by x-ray powder diffraction (XRPD) measurements (Supporting Information, Figure S1 b), the chlorination may easily involve also subsurface layers[27–29] and has a key role in the catalysis, both enhancing the Al^{3+} Lewis acidity[30] and

[*] A. Piovano, Dr. K. S. Thushara, Dr. E. Morra, Prof. M. Chiesa, Dr. E. Groppo
Department of Chemistry—INSTM and NIS Centre
University of Torino
via Giuria 7, 10125 Torino (Italy)
E-mail: elena.groppo@unito.it
Supporting information and the ORCID identification number(s) for the author(s) of this article can be found under http://dx.doi.org/10.1002/anie.201604136.

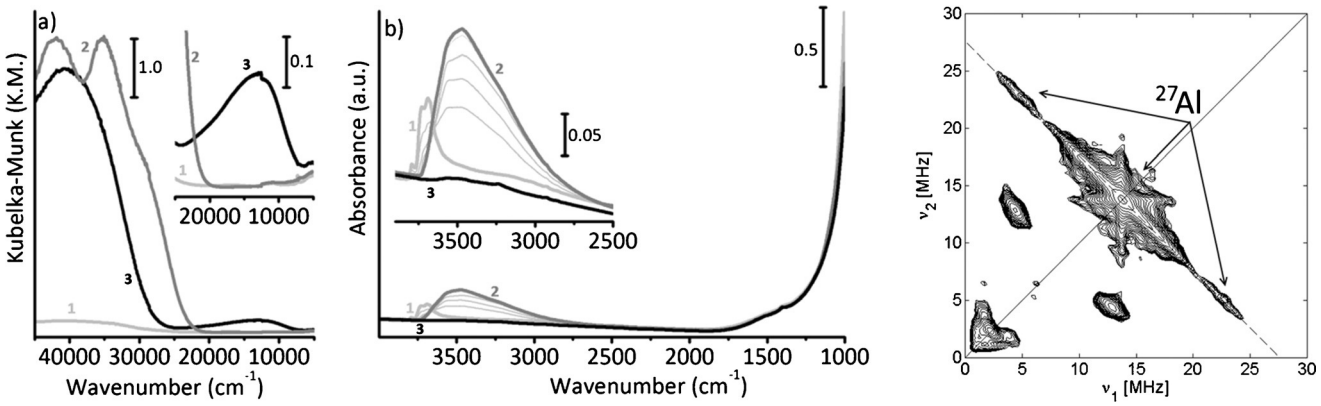

Figure 1. a) DR UV/Vis-NIR spectra of δ-$Al_2O_{3\text{-}600}$ support (1), δ-$Al_2O_{3\text{-}600}$/$TiCl_4$ pre-catalyst (2), and δ-$Al_2O_{3\text{-}600}$/$TiCl_4$/$H_{2\text{-}400}$ catalyst (3). Inset: Magnification of the d-d region. b) FT-IR spectra as in (a). The inset displays a magnification of the ν(OH) spectral region. Light gray spectra have been collected during pre-catalyst formation (from 1 to 2). c) Experimental Q-band HYSCORE spectrum, recorded at $T = 10$ K at observer position $B_0 = 1243.5$ mT corresponding to the maximum intensity of the ESE-detected EPR spectrum. HYSCORE spectra recorded at other field settings and computer simulations are reported in Figure S3 along with the Q-band ESE-EPR spectrum.

positively affecting the Ti^{3+} center activity.[31] The final amount of Ti present in the catalyst (approximately 2 wt%, as determined by ICP analysis) is in good agreement with that expected by considering the involvement of all the surface OH groups (approximately 4 OH/nm^2).

The local environment of the EPR active Ti^{3+} ions is revealed by hyperfine sublevel correlation (HYSCORE) experiments at Q band frequency (34.3 GHz), which allow detecting the NMR transitions of magnetically active nuclei in the vicinity of the paramagnetic center. A typical HYSCORE spectrum is shown in Figure 1 c. The spectrum is dominated by an extended ridge signal centered at 13.8 MHz (^{27}Al Larmor frequency at this field) with a maximum extension of approximately 21 MHz, arising from the hyperfine interaction of the unpaired electron localized on the Ti^{3+} with ^{27}Al nuclei of the alumina support. The ^{27}Al signal is consistent with a hyperfine interaction dominated by the isotropic Fermi contact contribution (a_{iso}),[32] ranging between 5 and 20 MHz (Table S1). Such isotropic couplings provide a unique and direct confirmation for the presence of Ti^{3+}–Cl–Al linkages, corresponding to a spin density transfer in the 3 s Al orbital in the range of 0.15–0.60 %, which is significantly larger than that observed for other systems involving M(3d^1)–L–Al linkages.[33]

The activity of the δ-$Al_2O_{3\text{-}600}$/$TiCl_4$/$H_{2\text{-}400}$ catalyst was tested for the gas-phase ethylene polymerization under very mild conditions (25 °C, $P_{C_2H_4} = 100$ mbar) and in the absence of any activator. Under these conditions the activity was evaluated at approximately 50 wt% of polymer on the catalyst, a value that can increase reasonably by two orders of magnitude by adopting industrial pressure and temperature conditions, as reported in Ref. [14]. The formation of polymer fibrils is directly observed by SEM (Figure 2 a,b). Size-exclusion chromatography (SEC) analysis (Figure 2 c and the Supporting Information, Table S3) indicates that the obtained product has a bimodal molecular weight distribution. The lighter fraction ($M_p \approx 360$ g mol^{-1}), which melts in the range of 115–125 °C and crystallizes at approximately 109 °C (Figure 2 d), is consistent with the polyethylene waxes

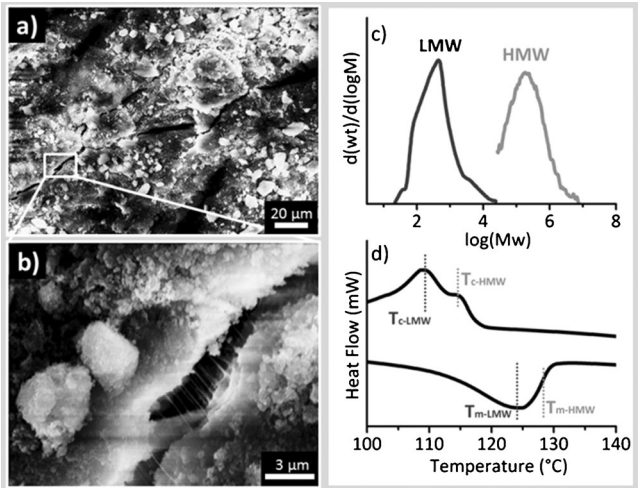

Figure 2. a), b) Representative SEM images of the polymer/catalyst mixture after ethylene polymerization. c) Molecular weight distribution of the polymeric product produced with the δ-$Al_2O_{3\text{-}600}$/$TiCl_4$/$H_{2\text{-}400}$ catalyst. d) Differential scanning calorimetry (DSC) curves of the polymer/catalyst mixture. LMW = low molecular weight, HMW = high molecular weight.

synthesized by ethylene oligomerization. The heavier fraction has a molecular weight typical for a polyethylene produced with traditional Ziegler–Natta catalysts ($M_p \approx 195\,000$ g mol^{-1}) and exhibits a melting temperature ($T_m = 128$ °C, Figure 2 d) characteristic of a branched polyethylene. The thermal and structural properties of the high molecular weight polymeric fraction are better appreciated in the analysis of the polymer extracted from the catalyst (Supporting Information, Figure S6). The bimodal mass weight distribution of the resulting products is a clear demonstration of the co-existence of dual active sites in the δ-$Al_2O_{3\text{-}600}$/$TiCl_4$/$H_{2\text{-}400}$ catalyst, in good agreement with the spectroscopic data. In addition, the branched nature of the high molecular weight polymeric fraction obtained with ethylene as the only feed, indicates that the two sites do not work independently.

Preliminary studies also revealed that temperature and pressure variations can change the relative abundance and the M_p of the two fractions, thus varying the length and the degree of the branching in the polymer.

To isolate the contribution of the reduced Ti^{3+} sites from that of the Al^{3+} Lewis acid sites, ethylene polymerization on the δ-$Al_2O_{3\text{-}600}$/$TiCl_4$/$H_{2\text{-}400}$ catalyst was monitored in situ by FT-IR spectroscopy (Figure 3b, and the Supporting Information, section 2.3) and compared with the FT-IR spectra of the ethylene reaction on chlorinated alumina, δ-$Al_2O_{3\text{-}600}$/$CCl_{4\text{-}400}$, as a reference (Figure 3a). Upon dosage of ethylene at 25 °C on δ-$Al_2O_{3\text{-}600}$/$CCl_{4\text{-}400}$ a complex series of absorption bands gradually rise in the 3000–2800 cm^{-1} and 1600–1300 cm^{-1} ranges (Figure 3a), indicating the formation and the limited growth of branched oligomers, along with allylic cationic species (band at 1535 cm^{-1}).[34] The reaction stops after approximately 30 min. Similar results were achieved by using $TiCl_4$ as a simple chlorinating agent in nonreductant conditions. Chlorinated alumina displays activity in acid-catalyzed reactions, such as olefin oligomerization[30,35,36] and double-bond shift isomerization,[37,38] involving a carbocationic mechanism. Moreover, AlX_3 Lewis acids are employed in industrial practice as initiators of carbocationic polymerization reactions,[39] in which propagation proceeds through repeated additions of ethylene to form the thermodynamically more stable carbocations (secondary and tertiary), which may migrate well away from the site of the initial attack.[40] Strong Lewis acids (such as chlorinated alumina) can stabilize carbocations,[41] promoting intramolecular hydrogen-transfer reactions, with the consequent formation of allyl cationic species.[42]

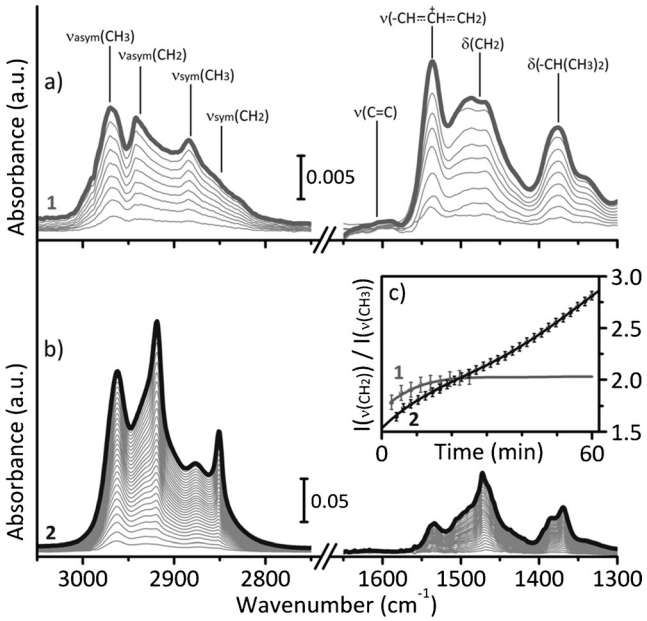

Figure 3. a) Background subtracted FT-IR spectra, in the ν(CH_x) and δ(CH_x) spectral regions, collected during ethylene oligo/polymerization (25 °C, $P_{C_2H_4}$ = 100 mbar) on the δ-$Al_2O_{3\text{-}600}$/$CCl_{4\text{-}400}$ catalyst. The whole sequence of spectra was collected in 25 min. b) the same as in (a) for the δ-$Al_2O_{3\text{-}600}$/$TiCl_4$/$H_{2\text{-}400}$ catalyst, collected in 1 h. Note that in (b) the absorbance scale is ten times the absorbance scale in (a). c) Evolution of the CH_2/CH_3 intensity ratio as a function of time, as determined from the intensity of the absorption bands at 2918 and 2962 cm^{-1} in the FT-IR spectra of both δ-$Al_2O_{3\text{-}600}$/$CCl_{4\text{-}400}$ (2) and δ-$Al_2O_{3\text{-}600}$/$TiCl_4$/$H_{2\text{-}400}$ catalysts (1). The ratio of the extinction coefficients $\varepsilon(CH_3)/\varepsilon(CH_2)$ was fixed to 2.2.[34]

A different spectral evolution is observed during the ethylene reaction on the δ-$Al_2O_{3\text{-}600}$/$TiCl_4$/$H_{2\text{-}400}$ catalyst (Figure 3b). At a short contact time, the FT-IR spectra are very similar to those previously discussed, but after approximately 15 min the absorption bands associated with the vibrational modes involving CH_2 groups start to grow faster than those related to the CH_3 groups. The ν(CH_2) absorption bands, which are sensitive indicators of the length of the alkyl chains,[43] slightly red-shift over time, indicating the formation of long linear polyethylene chains. The CH_2/CH_3 intensity ratio as a function of time has been used to roughly estimate the branching degree of the products during ethylene polymerization (Figure 3c). Both the catalysts show a similar behavior in the first 15 min, during which the acid-catalyzed formation of branched oligomers prevails. However, at a longer reaction time the CH_2/CH_3 ratio becomes increasingly higher for the δ-$Al_2O_{3\text{-}600}$/$TiCl_4$/$H_{2\text{-}400}$ catalyst, indicating that ethylene polymerization through a coordination mechanism is now taking place.[44]

The whole set of spectroscopic data shown above concur with the formation of bifunctional catalytic sites constituted by Ti^{3+} sites directly linked to strong Lewis acid Al^{3+} sites (Scheme 1a). The two sites exert specific functionalities,

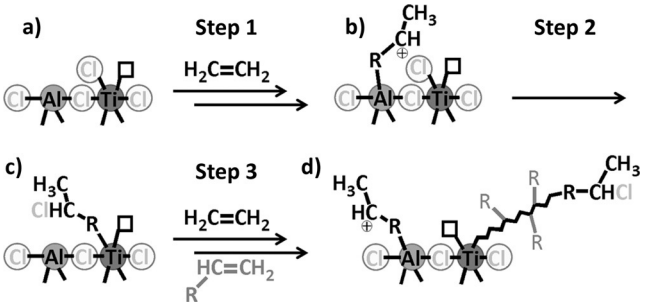

Scheme 1. Mechanism of ethylene conversion on the δ-$Al_2O_{3\text{-}600}$/$TiCl_4$/$H_{2\text{-}400}$ catalyst (where R stands for a branched oligomeric alkyl group). R–CH=CH_2 represents the branched oligomers produced by Al^{3+} sites by carbocationic polymerization. See text for details.

acting in a concerted fashion to synergistically boost the olefin conversion. The acid-catalyzed oligomerization of ethylene (Step 1 in Scheme 1) leads to the formation of branched cationic oligomers, stabilized by the presence of chloride ions on the catalyst surface (Scheme 1b). This step is necessary to activate the Ti^{3+} sites for ethylene coordination polymerization, since at the starting point they do not have alkyl ligands, as required by the widely accepted Cossee–Arlman mechanism.[45] Hence, the oligomers produced through a carbocationic mechanism on the Al^{3+} Lewis acid sites have the double function to dechlorinate and alkylate the Ti^{3+} sites (Step 2 in Scheme 1), as revealed by DR UV/Vis spectroscopy (Supporting Information, Figure S5).[46] Once the Ti sites are

alkylated (Scheme 1c), ethylene polymerization takes place through the repeated insertion of the monomer and the simultaneous enchainment of the branched oligomers promoted by the Al^{3+} sites (Step 3 in Scheme 1), accounting for the production of a branched polyethylene (Scheme 1d).

In summary, the synergistic cooperation between Ti^{3+} and Al^{3+} sites on a chlorinated Al_2O_3 in tandem olefin conversion was confirmed for the first time, thanks to a multi-technique approach, which opens interesting perspectives not only in the field of olefin polymerization catalysis, but more generally in the investigation of tandem heterogeneous catalysts.

Acknowledgements

We are grateful to Jarmo Lindroos (Norner AS) for SEC measurements and the useful advice on the polymer analysis, and to Adriano Zecchina and Silvia Bordiga for enlightening discussions. This work has been supported by the Progetto di Ateneo/CSP 2014 (Torino call2014 L1 73).

Keywords: EPR spectroscopy · operando FT-IR spectroscopy · tandem catalysis · Ti^{3+} sites · Ziegler–Natta catalysts

How to cite: *Angew. Chem. Int. Ed.* **2016**, *55*, 11203–11206
Angew. Chem. **2016**, *128*, 11369–11372

[1] Z. J. A. Komon, G. C. Bazan, *Macromol. Rapid Commun.* **2001**, *22*, 467.
[2] M. Frediani, C. Fiel, W. Kaminsky, C. Bianchini, L. Rosi, *Macromol. Symp.* **2006**, *236*, 124.
[3] T. L. Lohr, T. J. Marks, *Nat. Chem.* **2015**, *7*, 477.
[4] M. J. Climent, A. Corma, S. Iborra, M. J. Sabater, *ACS Catal.* **2014**, *4*, 870.
[5] R. W. Barnhart, G. C. Bazan, T. Mourey, *J. Am. Chem. Soc.* **1998**, *120*, 1082.
[6] M. Frediani, C. Bianchini, W. Kaminsky, *Kinet. Catal.* **2006**, *47*, 207.
[7] D. Cicmil, J. Meeuwissen, A. Vantomme, J. Wang, I. K. Van Ravenhorst, H. E. Van Der Bij, A. Muñoz-Murillo, B. M. Weckhuysen, *Angew. Chem. Int. Ed.* **2015**, *54*, 13073; *Angew. Chem.* **2015**, *127*, 13265.
[8] C. Robert, C. M. Thomas, *Chem. Soc. Rev.* **2013**, *42*, 9392.
[9] H. Li, T. J. Marks, *Proc. Natl. Acad. Sci. USA* **2006**, *103*, 15295.
[10] M. Delferro, T. J. Marks, *Chem. Rev.* **2011**, *111*, 2450.
[11] T. Vestberg, P. Denifl, M. Parkinson, C. E. Wilén, *J. Polym. Sci. Part A* **2010**, *48*, 351.
[12] M. P. McDaniel, *Adv. Catal.* **2010**, *53*, 123.
[13] C. Barzan, D. Gianolio, E. Groppo, C. Lamberti, V. Monteil, E. A. Quadrelli, S. Bordiga, *Chem. Eur. J.* **2013**, *19*, 17277.
[14] C. L. Thomas, US 3255167 A, **1966**.
[15] J. Inomata, K. Iwasaki, G. Kakogawa, S. Kamimura, R. Matsuura, K. Yamaguchi, US 3506633 A, **1970**.
[16] E. Groppo, K. Seenivasan, C. Barzan, *Catal. Sci. Technol.* **2013**, *3*, 858.
[17] J. B. Kinney, R. H. Staley, *J. Phys. Chem.* **1983**, *87*, 3735.
[18] S. Haukka, E. L. Lakomaa, O. Jylha, J. Vilhunen, S. Hornytzkyj, *Langmuir* **1993**, *9*, 3497.
[19] S. Haukka, E. L. Lakomaa, A. Root, *J. Phys. Chem.* **1993**, *97*, 5085.
[20] A. Kytokivi, S. Haukka, *J. Phys. Chem. B* **1997**, *101*, 10365.
[21] K. Seenivasan, E. Gallo, A. Piovano, J. G. Vitillo, A. Sommazzi, S. Bordiga, C. Lamberti, P. Glatzel, E. Groppo, *Dalton Trans.* **2013**, *42*, 12706.
[22] A. R. McInroy, D. T. Lundie, J. M. Winfield, C. C. Dudman, P. Jones, S. F. Parker, D. Lennon, *Catal. Today* **2006**, *114*, 403.
[23] K. Seenivasan, A. Sommazzi, F. Bonino, S. Bordiga, E. Groppo, *Chem. Eur. J.* **2011**, *17*, 8648.
[24] C. K. Jorgensen, in *Orbitals in Atoms and Molecules*, Academic Press, London and New York, **1962**, pp. 80.
[25] C. K. Jorgensen, *Prog. Inorg. Chem.* **1970**, *12*, 101.
[26] E. Morra, E. Giamello, S. Van Doorslaer, G. Antinucci, M. D′Amore, V. Busico, M. Chiesa, *Angew. Chem. Int. Ed.* **2015**, *54*, 4857; *Angew. Chem.* **2015**, *127*, 4939.
[27] A. Krzywicki, M. Marczewski, *J. Chem. Soc. Faraday Trans. 1* **1980**, *76*, 1311.
[28] A. Kytökivi, M. Lindblad, A. Root, *J. Chem. Soc. Faraday Trans.* **1995**, *91*, 941.
[29] A. Khaleel, B. Dellinger, *Environ. Sci. Technol.* **2002**, *36*, 1620.
[30] A. Corma, H. Garcia, *Chem. Rev.* **2003**, *103*, 4307.
[31] T. Tsujino, A. Kaiya, N. Kuroda, M. Takahashi, *J. Macromol. Sci. Chem. A* **1971**, *5*, 311.
[32] A. Pöppl, L. Kevan, *J. Phys. Chem.* **1996**, *100*, 3387.
[33] S. Maurelli, G. Berlier, M. Chiesa, F. Musso, F. Corà, *J. Phys. Chem. C* **2014**, *118*, 19879.
[34] M. Bjørgen, K. P. Lillerud, U. Olsbye, S. Bordiga, A. Zecchina, *J. Phys. Chem. B* **2004**, *108*, 7862.
[35] C. T. O'Connor, M. Kojima, *Catal. Today* **1990**, *6*, 329.
[36] S. Aoshima, S. Kanaoka, *Chem. Rev.* **2009**, *109*, 5245.
[37] J. H. Lunsford, L. W. Zingery, M. P. Rosynek, *J. Catal.* **1975**, *38*, 179.
[38] A. Ayame, G. Sawada, *Bull. Chem. Soc. Jpn.* **1989**, *62*, 3055.
[39] F. J. Chen, H. Cheradame, J. E. Stanat, G. Rissoan, US 5874380 A, **1999**.
[40] M. C. Baird, *Chem. Rev.* **2000**, *100*, 1471.
[41] G. A. Olah, *J. Org. Chem.* **2001**, *66*, 5943.
[42] A. Ayame, G. Sawada, H. Sato, G. Zhang, T. Ohta, T. Izumizawa, *Appl. Catal.* **1989**, *48*, 25.
[43] E. Groppo, C. Lamberti, G. Spoto, S. Bordiga, G. Magnacca, A. Zecchina, *J. Catal.* **2005**, *236*, 233.
[44] E. Groppo, K. Seenivasan, E. Gallo, A. Sommazzi, C. Lamberti, S. Bordiga, *ACS Catal.* **2015**, *5*, 5586.
[45] P. Cossee, *J. Catal.* **1964**, *3*, 80.
[46] It is worth noticing that analogous systems where $TiCl_x$ species are grafted on non-acidic supports are not active in ethylene polymerization when just reduced by H_2 at similar temperature conditions.

Received: April 28, 2016
Revised: June 14, 2016
Published online: July 21, 2016

